

Weak Fermi Level Pinning and Low Barrier Interfacial Contact: 2D Lead-free Perovskite on Multilayer GaN

Pengjie Fu, Baolin Wang, Mengni Liu, Guixian Ge, Juan Hou,* and Xiaodong Yang*

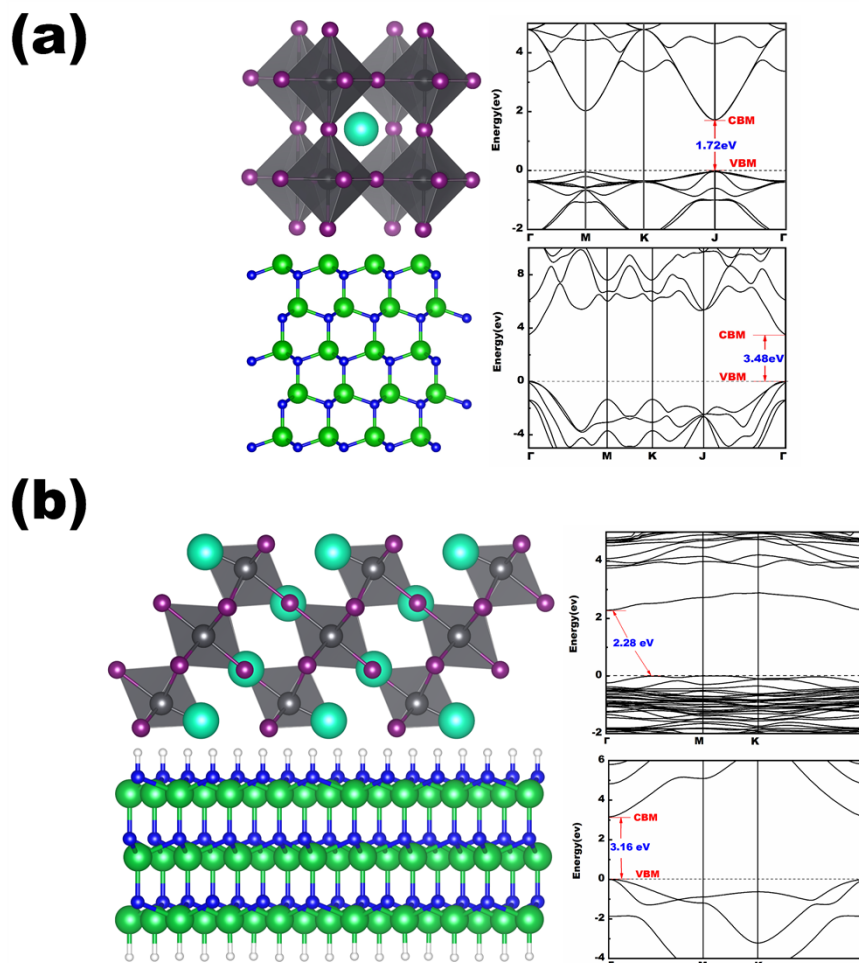


Fig. S1. Structures and band gaps of (a) bulk CsPbI₃ and GaN, (b) 2D CsPbI₃ and GaN. The zero of the Fermi energy is set at VBM.

Table S1. The band gaps of CsPbI₃ and GaN calculated using different methods. For the comparison, previous reports on the band gaps of CsPbI₃ and GaN were also listed.

E _g (eV)	PBE	SOC	HSE+SOC	Meta-GGA	Previous works
CsPbI ₃	1.408	1.503	1.652	1.716	1.67 ¹ , 1.73 ²
GaN	1.634	1.691	3.378	3.477	3.39 ³ , 3.47 ⁴

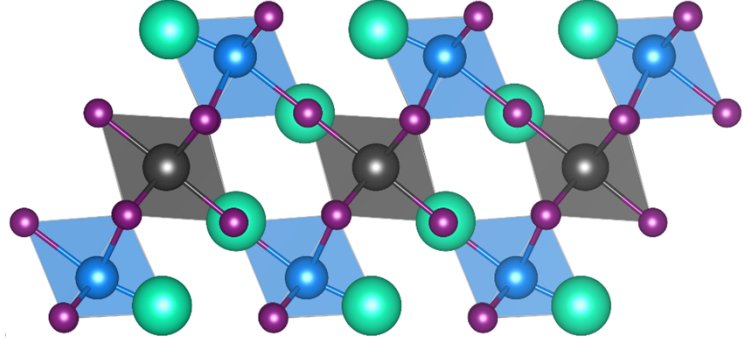


Fig. S2. Structure of M-CsPbI₃ (M=Sb, Bi, In) passivated with different metallic elements, respectively.

Table S2. Surface energies (γ_s) of M-CsPbI₃ (M= Pb, Sb, Ln and Bi) nanosheets.

	CsPbI ₃	Sb-CsPbI ₃	Ln-CsPbI ₃	Bi-CsPbI ₃
γ_s (meV/Å ²)	43.52	-19.55	35.74	38.16

$$\gamma_s = \frac{E_T - n_v E_{CsPbI_3} + \sum \Delta n_M \mu_M}{2A} \quad (S1)$$

where E_T and E_{CsPbI_3} are total energies of 2D M-CsPbI₃ nanosheets and CsPbI₃ in cubic bulk, respectively. A is the surface area of nanosheets, n_v is the number of CsPbI₃ formula unit in 2D nanosheets, μ_M is the chemical potential of atomic species M (M = Pb, Sb, In and Bi), and Δn_M is the difference of atom numbers between the given 2D structure and n_v bulk CsPbI₃.

Table S3. Surface energies (γ_s) of [M₁]-CsSrI₃ (M₁= Ba, Sn, Sr, Mg, Ca, Zn, Cu) nanosheets.

	Ba	Sn	Sr	Mg	Ca	Zn	Cu
γ_s (meV/Å ²)	-32.44	-19.55	-12.57	35.12	28.77	38.15	40.26

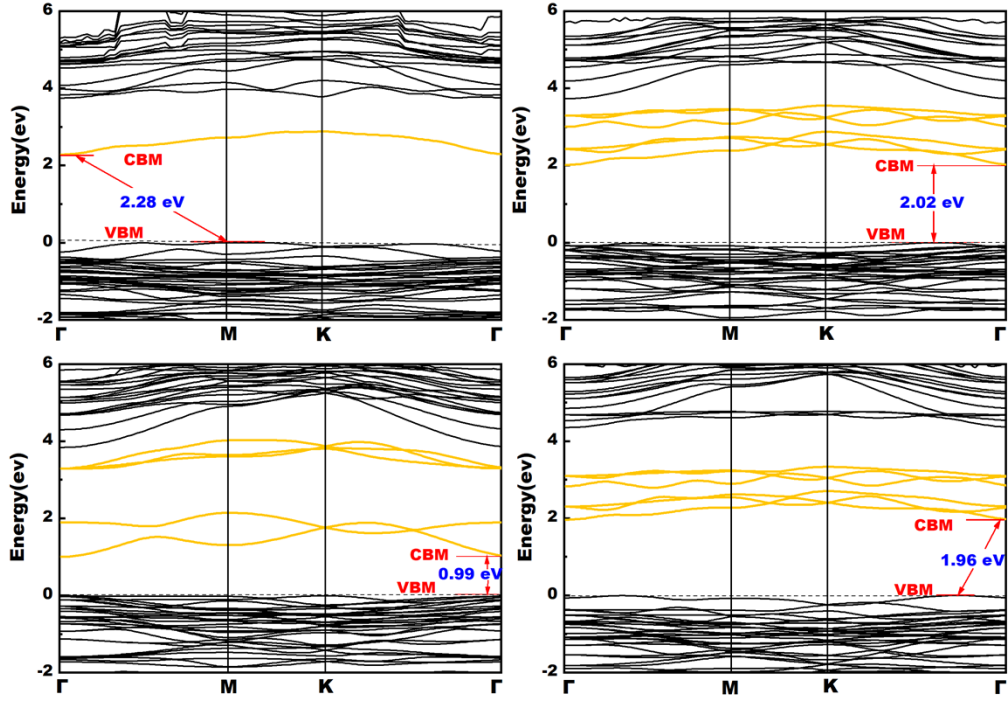


Fig. S3. Band gaps of $[M_1]$ -CsSrI₃ (M_1 =Sn, Mg, Ca, Zn) passivated with different metallic elements (a) Sn, (b) Mg, (c) Ca and (d) Zn, respectively. The zero of the Fermi energy is set at VBM. The orange lines represent impurity energy levels.

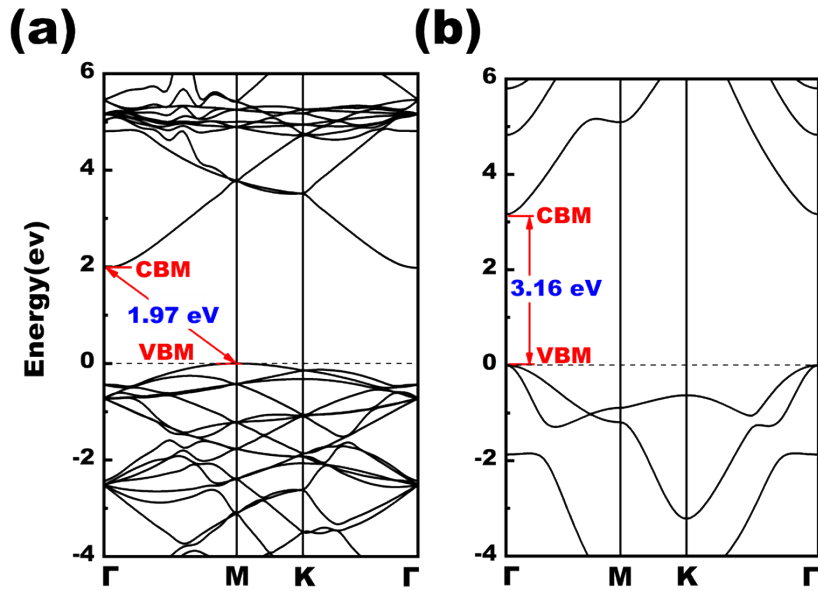


Fig. S4. Band structures of (a) non-passivated and (b) passivated GaN.

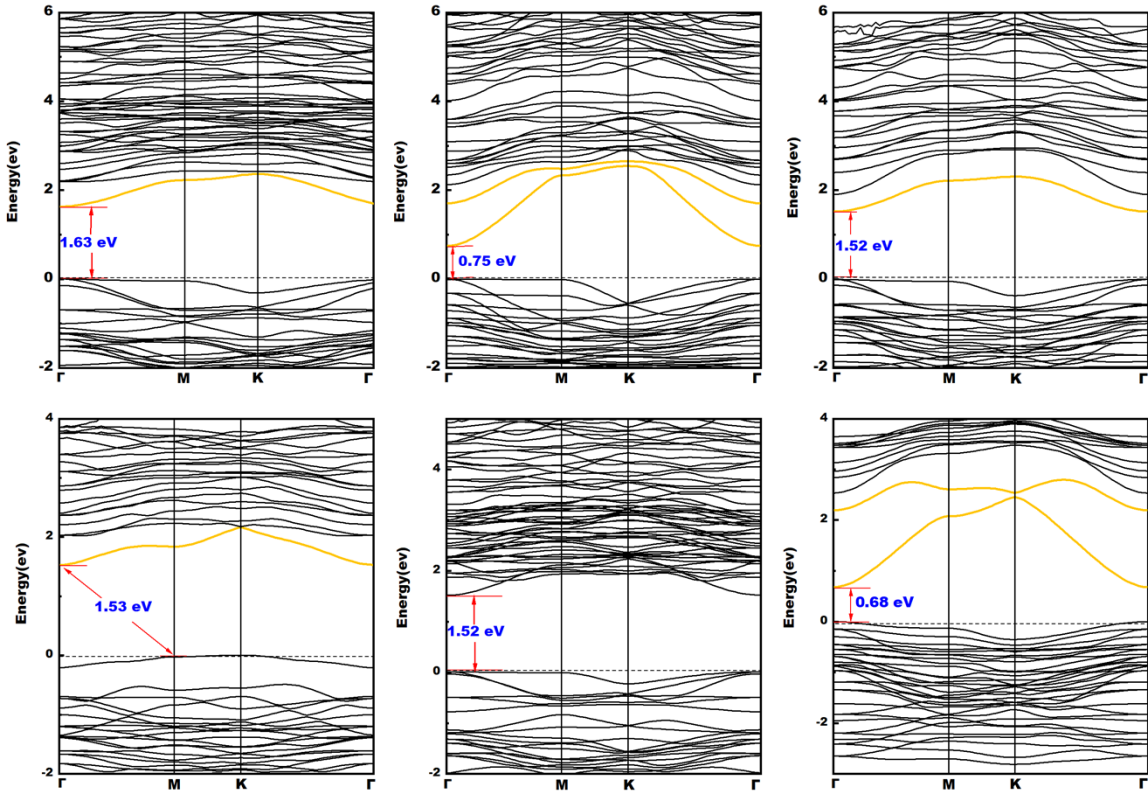


Fig. S5. Band structures of 2D perovskite/GaN heterostructures are obtained by the replacement of Sr²⁺ in Ba-CsSrI₃/GaN with (a) Sn²⁺, (b) Cu²⁺, (c) Mg²⁺, (d) Ca²⁺, (e) Ba²⁺ and (f) Zn²⁺, respectively. The orange lines represent impurity energy levels.

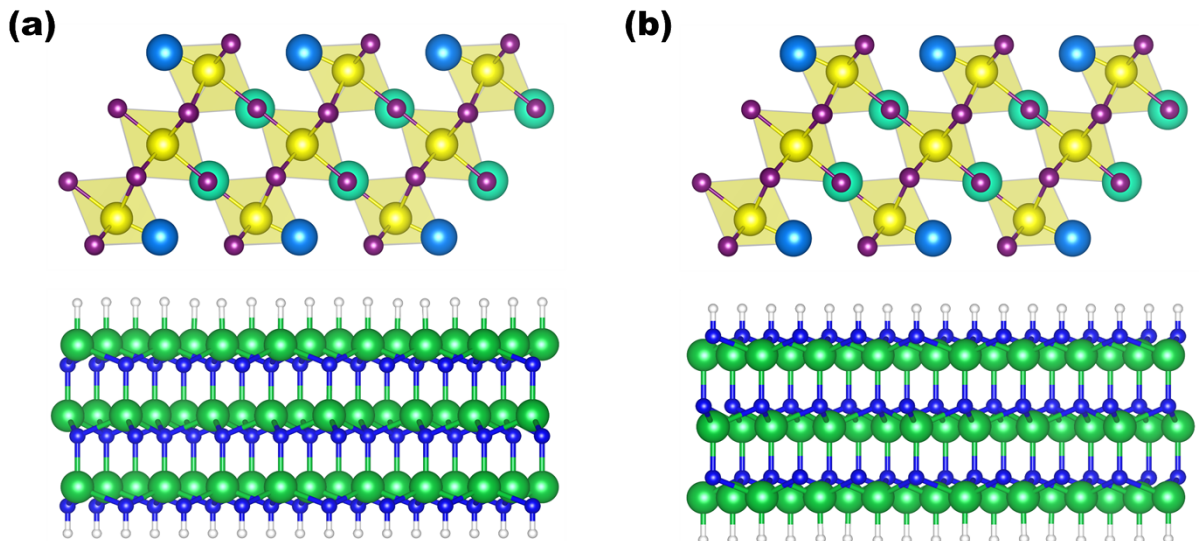


Fig. S6. The structure diagrams of the two Ba-CsSrI₃/GaN heterojunction with (a) Ga-top and (b) N-top configurations.

Table S4. Elastic stiffness constants C_{ij} and stability of Ba-CsSrI₃/GaN heterostructures with different interfacial configurations.

	C_{11}	C_{12}	C_{13}	C_{14}	C_{15}	C_{16}	C_{21}	C_{22}	C_{23}	C_{24}	C_{25}	C_{26}
Ga-top	581.05	215.26	44.62	-14.54	-19.25	17.43	215.26	621.88	57.96	-8.71	-10.21	2.81
	C_{31}	C_{32}	C_{33}	C_{34}	C_{35}	C_{36}	C_{41}	C_{42}	C_{43}	C_{44}	C_{45}	C_{46}
	44.62	57.96	145.16	-0.89	-5.41	4.54	-14.54	-8.71	-0.89	193.27	-15.06	9.65
	C_{51}	C_{52}	C_{53}	C_{54}	C_{55}	C_{56}	C_{61}	C_{62}	C_{63}	C_{64}	C_{65}	C_{66}
	-19.25	-10.21	-5.41	-15.06	34.32	4.84	17.43	2.81	4.54	9.65	4.84	42.66
	C_{11}	C_{12}	C_{13}	C_{14}	C_{15}	C_{16}	C_{21}	C_{22}	C_{23}	C_{24}	C_{25}	C_{26}
N-top	122.17	127.96	34.95	38.64	16.57	14.22	127.96	14.78	13.58	-2.48	2.21	-2.61
	C_{31}	C_{32}	C_{33}	C_{34}	C_{35}	C_{36}	C_{41}	C_{42}	C_{43}	C_{44}	C_{45}	C_{46}
	34.95	13.58	21.48	14.27	6.56	26.11	38.64	-2.48	14.27	15.34	4.59	3.42
	C_{51}	C_{52}	C_{53}	C_{54}	C_{55}	C_{56}	C_{61}	C_{62}	C_{63}	C_{64}	C_{65}	C_{66}
	16.57	2.21	6.56	4.59	9.81	43.53	14.22	-2.61	26.11	3.42	43.53	7.33
	C_{11}	C_{12}	C_{13}	C_{14}	C_{15}	C_{16}	C_{21}	C_{22}	C_{23}	C_{24}	C_{25}	C_{26}

Taking Ba-CsSrI₃/GaN heterostructures as an example, both configurations have the triclinic symmetry, resulting in thirty-six independent elastic constants as follows⁵

$$C = \begin{pmatrix} C_{11} & C_{12} & C_{13} & C_{14} & C_{15} & C_{16} \\ C_{21} & C_{22} & C_{23} & C_{24} & C_{25} & C_{26} \\ C_{31} & C_{32} & C_{33} & C_{34} & C_{35} & C_{36} \\ C_{41} & C_{42} & C_{43} & C_{44} & C_{45} & C_{46} \\ C_{51} & C_{52} & C_{53} & C_{54} & C_{55} & C_{56} \\ C_{61} & C_{62} & C_{63} & C_{64} & C_{65} & C_{66} \end{pmatrix} \quad (S2)$$

First-order: $C_{11} > 0$

Second-order: $C_{11}C_{22}-C_{12}^2 > 0$

Third-order: $C_{11}C_{22}C_{33}+2C_{12}C_{13}C_{23}-C_{11}C_{23}^2-C_{22}C_{13}^2-C_{33}C_{12}^2 > 0$

Fourth-order: $C_{11}(C_{22}C_{33}C_{44}+2C_{23}C_{24}C_{34}-C_{33}C_{24}^2-C_{22}C_{34}^2-C_{44}C_{23}^2)-C_{12}(C_{12}C_{33}C_{44}+C_{23}C_{14}C_{34}+C_{13}C_{24}C_{34}-C_{33}C_{14}C_{24}-C_{12}C_{34}^2-C_{13}C_{23}C_{44})+C_{13}(C_{12}C_{23}C_{44}+C_{22}C_{14}C_{34}+C_{13}C_{24}^2-C_{23}C_{14}C_{34}^2-C_{12}C_{24}C_{34}-C_{22}C_{13}C_{44})-C_{14}(C_{12}C_{23}C_{34}+C_{22}C_{33}C_{14}+C_{13}C_{23}C_{24}-C_{14}C_{23}^2-C_{12}C_{33}C_{24}-C_{22}C_{13}C_{34}) > 0$

Fifth-order: $C_{11}(a-b+c-d)-C_{12}(e-f+g-h)+C_{13}(i-j+k-l)-C_{14}(m-n+o-p)+C_{15}(q-r+s-t) > 0$

$$\sum_{i=1}^{20} A_i B_i > 0$$

Sixth-order:

Among:

$$a = C_{22}(C_{33}C_{44}C_{55}+2C_{34}C_{35}C_{45}-C_{44}C_{35}^2-C_{33}C_{45}^2-C_{55}C_{34}^2)$$

$$b = C_{23}(C_{23}C_{44}C_{55}+C_{34}C_{25}C_{45}+C_{24}C_{35}C_{45}-C_{44}C_{25}C_{35}-C_{23}C_{45}^2-C_{24}C_{34}C_{55})$$

$$\begin{aligned}
c &= C_{24}(C_{23}C_{34}C_{55} + C_{33}C_{45}C_{25} + C_{24}C^2_{35} - C_{34}C_{25}C_{35} - C_{23}C_{35}C_{45} - C_{33}C_{24}C_{55}) \\
d &= C_{25}(C_{23}C_{34}C_{45} + C_{33}C_{44}C_{25} + C_{24}C_{34}C_{35} - C^2_{34}C_{25} - C_{23}C_{44}C_{35} - C_{33}C_{24}C_{45}) \\
e &= C_{12}(C_{33}C_{44}C_{55} + 2C_{34}C_{35}C_{45} - C_{44}C^2_{35} - C_{33}C^2_{45} - C_{55}C^2_{34}) \\
f &= C_{23}(C_{13}C_{44}C_{55} + C_{34}C_{15}C_{45} + C_{14}C_{35}C_{45} - C_{44}C_{15}C_{35} - C_{13}C^2_{45} - C_{14}C_{34}C_{55}) \\
g &= C_{24}(C_{13}C_{34}C_{55} + C_{33}C_{45}C_{15} + C_{14}C^2_{35} - C_{34}C_{15}C_{35} - C_{13}C_{35}C_{45} - C_{33}C_{14}C_{55}) \\
h &= C_{25}(C_{13}C_{34}C_{45} + C_{33}C_{44}C_{15} + C_{14}C_{34}C_{35} - C^2_{34}C_{15} - C_{13}C_{44}C_{35} - C_{33}C_{14}C_{45}) \\
i &= C_{12}(C_{23}C_{44}C_{55} + C_{34}C_{25}C_{45} + C_{24}C_{35}C_{45} - C_{44}C_{25}C_{35} - C_{23}C^2_{45} - C_{24}C_{34}C_{55}) \\
j &= C_{22}(C_{13}C_{44}C_{55} + C_{34}C_{15}C_{45} + C_{14}C_{35}C_{45} - C_{44}C_{15}C_{35} - C_{13}C^2_{45} - C_{14}C_{34}C_{55}) \\
k &= C_{24}(C_{13}C_{24}C_{55} + C_{23}C_{15}C_{45} + C_{14}C_{25}C_{35} - C_{24}C_{15}C_{35} - C_{13}C_{25}C_{45} - C_{23}C_{14}C_{55}) \\
l &= C_{25}(C_{13}C_{24}C_{45} + C_{23}C_{44}C_{15} + C_{14}C_{34}C_{25} - C_{24}C_{34}C_{15} - C_{13}C_{44}C_{25} - C_{23}C_{14}C_{45}) \\
m &= C_{12}(C_{23}C_{34}C_{55} + C_{33}C_{25}C_{45} + C_{24}C^2_{35} - C_{34}C_{25}C_{35} - C_{23}C_{35}C_{45} - C_{33}C_{24}C_{55}) \\
n &= C_{22}(C_{13}C_{34}C_{55} + C_{33}C_{15}C_{45} + C_{14}C^2_{35} - C_{34}C_{15}C_{35} - C_{13}C_{35}C_{45} - C_{33}C_{14}C_{55}) \\
o &= C_{23}(C_{13}C_{24}C_{55} + C_{23}C_{45}C_{15} + C_{14}C_{25}C_{35} - C_{24}C_{15}C_{35} - C_{13}C_{25}C_{45} - C_{23}C_{14}C_{55}) \\
p &= C_{25}(C_{13}C_{24}C_{35} + C_{23}C_{34}C_{15} + C_{33}C_{14}C_{25} - C_{33}C_{24}C_{15} - C_{13}C_{34}C_{25} - C_{23}C_{14}C_{35}) \\
q &= C_{12}(C_{23}C_{34}C_{45} + C_{33}C_{44}C_{25} + C_{24}C_{34}C_{35} - C_{25}C^2_{34} - C_{23}C_{44}C_{35} - C_{24}C_{33}C_{45}) \\
r &= C_{22}(C_{13}C_{34}C_{45} + C_{33}C_{44}C_{15} + C_{14}C_{34}C_{35} - C_{15}C^2_{34} - C_{13}C_{44}C_{35} - C_{33}C_{14}C_{45}) \\
s &= C_{23}(C_{13}C_{24}C_{45} + C_{23}C_{44}C_{15} + C_{14}C_{25}C_{34} - C_{34}C_{24}C_{15} - C_{13}C_{25}C_{44} - C_{14}C_{23}C_{45}) \\
t &= C_{24}(C_{13}C_{24}C_{35} + C_{23}C_{34}C_{15} + C_{14}C_{25}C_{33} - C_{33}C_{24}C_{15} - C_{13}C_{34}C_{25} - C_{23}C_{14}C_{35})
\end{aligned}$$

Table S5. Surface energies (γ_s) of GaN (n=1,2,3,4,5,6) nanosheets.

Number of GaN layers (n)	n=1	n=2	n=3	n=4	n=5	n=6
γ_s (meV/Å ²)	-43.274	-47.153	-47.341	-47.344	-47.344	-47.345

Table S6. Formation energy E_f of Ga-top Cs₂Ba₂Sr₃I₁₂/GaN (n=1,2,3,4,5,6).

Number of GaN layers (n)	n=1	n=2	n=3	n=4	n=5	n=6
E_f (eV/Å ²)	-0.211	-0.234	-0.261	-0.263	-0.264	-0.266

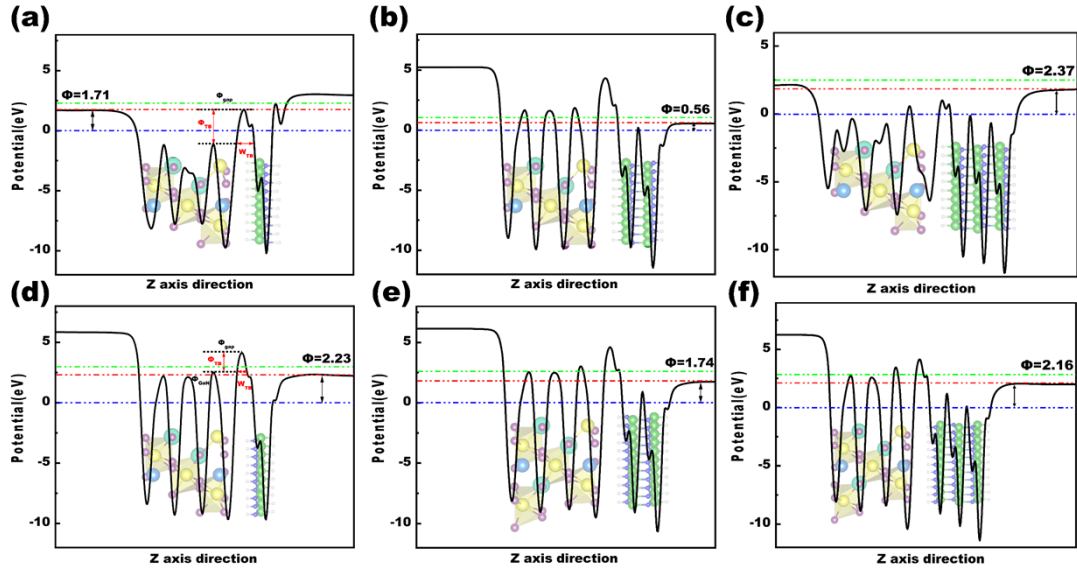


Fig. S7. Electrostatic potential distributions of 2D Ba-CsSrI₃/GaN heterostructures. Electrostatic potentials of (a) Ga-top($n=1$), (b) Ga-top($n=2$). (c) Ga-top($n=3$). Electrostatic potential of (d) N-top($n=1$), (e) N-top($n=2$), (f) N-top($n=3$). Vacuum level, CBM, and Fermi level are indicated by red, blue, and green lines in electrostatic potential distributions, respectively.

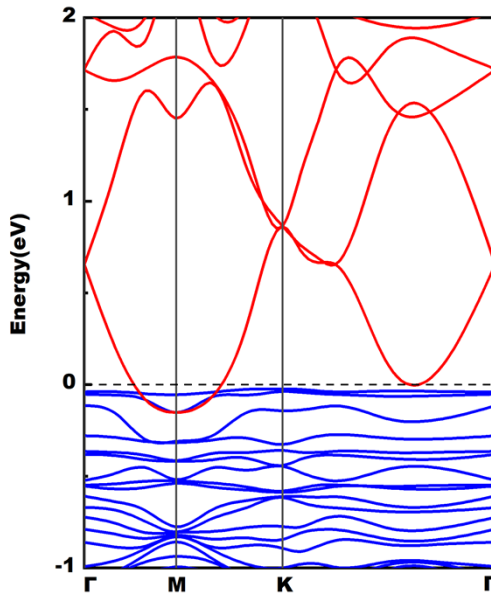


Fig. S8. The band structure of the Ba-CsSrI₃/GaN ($n=3$) heterojunction with Ga-top configuration.

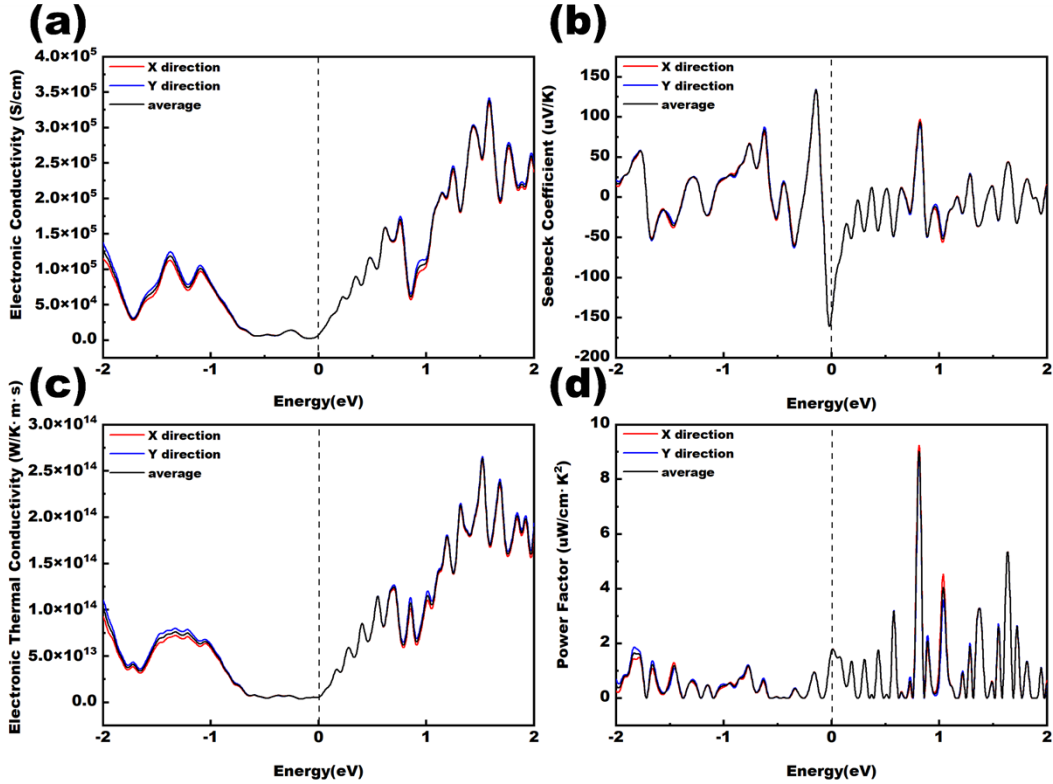


Fig. S9. (a) Electronic conductivity (b) Seebeck coefficient (c) electronic thermal conductivity (d) power factor of Ba-CsSrI₃/GaN (n=3) heterojunction.

The relaxation time τ is required to calculate the electrical conductivity. By utilizing the deformation potential (DP) theory, in combined with the effective mass approximation, the τ can be calculated as⁶

$$\tau = \frac{um^*}{\mathcal{C}} = \frac{2\hbar^3 C}{3k_B T m^* E} \quad (\text{S3})$$

$$C = [\partial^2 E / \partial(\Delta a/a_0)^2] / S_0 \quad (\text{S4})$$

where C is the elastic constant, \mathcal{C} is the deformation potential energy, m^* is the effective mass, u is the mobility of carriers, including electrons and holes, \hbar is the reduced Planck constant, T is the temperature, E is the total energy of the system. Δa is the change of the lattice constant, $\Delta a/a_0$ is the magnitude of the uniaxial stress, and S_0 is the bottom area of the two-dimensional material.

REFERENCES

- (1) Xiao, Z.; Meng, W.; Wang, J.; Mitzi, D. B.; Yan, Y. Searching for promising new perovskite-based photovoltaic absorbers: the importance of electronic dimensionality. Mater. Horiz. 4 (2017)

206-216.

- (2) Swarnkar. A.; Marshall, A. R.; Sanehira, E. M.; Chernomordik, B. D.; Moore, D. T.; Christians, J. A.; Chakrabarti, T.; Luther, J. M. Quantum dot-induced phase stabilization of α -CsPbI₃ perovskite for high-efficiency photovoltaics. *Science*. 354 (2016) 92-95.
- (3) Levinshtein, M. E.; Rumyantsev, S. L.; Shur, M.; S. Properties of advanced semiconductor materials: GaN, AlN, InN, BN, SiC, SiGe. John Wiley & Sons: U.K. 2001.
- (4) Abd, E. H.; Ismail, Y.; Deen, M. J. A computational study of nonparabolic conduction band effect on quantum wire transport (eg GaN). *Opt. Quantum Electron.* 45 (2013) 885-899.
- (5) Gao, J.; Liu, Q.; Jiang, C.; Fan, D.; Zhang, M.; Liu, F.; Tang, B. The mechanical stability criterion of 7 large crystal system and its application: taking SiO₂ as an example. *Chin. J. High Press. Phys.* 36 (2022) 051101.
- (6) Bardeen, J.; Shockley, W. J. P. R. Deformation potentials and mobilities in non-polar crystals. *Phys. Rev.* 80 (1950) 72.